Journal of Environmental Science Studies; Vol. 7, No. 2, 2024
ISSN 2591-779X E-ISSN 2630-4821
Published by July Press

Experimental Investigation on Velocity Field in Subterranean Water Flow Under Different Size of Gravel

Youichi Yasuda[1] & Megumi Uemura[2]

[1] Department of Civil Engineering, College of Science and Technology, Nihon University, Tokyo, Japan

[2] Department of Civil Engineering, Gradual School of Science and Technology, Nihon University, Tokyo, Japan

Correspondence: Prof. Youichi Yasuda, Civil Engineering Dept., College of Sci. and Tech., Nihon University, Tower Schola S1011, 1-8-14 Kanda Surugadai, Chiyoda-ku, 101-8308 Tokyo. E-mail: yasuda.youichi@nihon-u.ac.jp

Received: June 26, 2024 Accepted: July 27, 2024 Online Published: November 23, 2024

doi:10.20849/jess.v7i2.1460 URL: https://doi.org/10.20849/jess.v7i2.1460

Abstract

Direct measurement of flow velocities within subterranean layer is important for predicting subterranean flow. The authors conducted a study on the velocity field of subterranean water flow by directly measuring the flow velocity within the subterranean layer using crushed stone to form a gravel mount. Namely, they directly measured subterranean flow velocities for five different sizes of gravels (5.3 mm, 16.5 mm, 25.5 mm, 47.5 mm, and 92.4 mm) and showed for the first time how the time-averaged flow velocity and standard deviation vary with the size of the gravels. The velocity field including turbulent intensity in the subterranean layer was revealed, and the flow field of the subterranean flow depends on the size of the gravels that make up the gravel mount. The relationship between the configuration of the gravel mount, the water surface profile, and the velocity field within the subterranean layer allowed a discussion of the vertical distribution of time-averaged velocities and standard deviations, as well as stream wise changes in the subterranean layer. From the results of time-averaged velocity and turbulent intensity (here, standard deviation) in the subterranean layer for different sizes of gravels, it is possible to estimate the velocity field of subterranean water flow formed by the grain size distribution of the depositing gravels and the difference in water level. In other words, by clarifying the velocity field of subterranean water flow consisting of different gravel sizes, it may be possible to evaluate the subterranean function of the sand and gravel zone deposited by transported gravels.

Keywords: seepage flow, gravel mount, assembled boulders, subterranean layer

1. Introduction

The formation of gravel zone with subterranean stream is important for the preservation of habitat and spawning habitat for multi-aquatic animals in rivers. It can be observed that subterranean stream water is generated through the difference of water level caused by the sedimentary sand and gravel zone in meandering areas of rivers. In large area of the sedimentary sand and gravel zone, the formation of subterranean stream might help for regulating water temperature, which is an important function for the spawning environment. In addition, during summer droughts, subterranean water does not lead to an abnormal increase in water temperature. Previous studies have shown the importance of subterranean stream water and underground water for ecosystem conservation (Orchard, 1988, Wheaton et al. 2004, Schirmer et al. 2013, Kawanishi, and Inoue, 2018, Piccoli and Yasuda, 2023, Yasuda et al. 2024). There are also examples of studies analyzing seepage flow around dikes and crossing structures including weirs (Zhang and Chanson, 2015 and Fukuoka and Tabata, 2018). However, there are few examples of studies on the systematic creation of subterranean functions to contribute to aquatic ecosystems. Although there have been studies on velocity fields in subterranean flows (Wroblicky et al. 1998, Han et al. 2020, Ghasemizade and Schirmer, 2013, Nagai et al. 2013), there is no indication from other researchers to consider velocities including turbulence in the subterranean layer.

Regarding direct measurement of time series changes in velocities within the subterranean layer, as a first step, the authors conducted a study on subterranean water flow by using crushed stones in the form of gravel mount (Yasuda and Uemura, 2023). They showed for the first time the velocity field including turbulence in the subterranean water flow. Considering the several sizes of gravels, the flow field of the subterranean flow may differ depending on the size of the gravels that make up the gravel mount. In order to contribute to the

improvement of the river environment, it is necessary to expand the range of gravel size considerations and to investigate the velocity fields within the subterranean flow. By elucidating the velocity field of the subterranean flow composed of different gravel sizes, it might be possible to evaluate the subterranean flow function in the sand and gravel zones deposited by transported gravels. In this paper, the authors measured velocities in the subterranean water flow directly for gravels of 5.3 mm, 16.5 mm, 25.5 mm, 47.5 mm, and 92.4 mm averaged in size, and clarified how the time-averaged velocity and standard deviation varied with gravel size.

2. Experimental Setup

Experiments were conducted in a horizontal rectangular channel of 15 m long, 60 cm height, and 40 cm width with both side walls made of tempered glass, a gravel mount was installed in the channel (Photo 1). The experimental conditions are shown in Table 1. The surface part of the gravel mount was constructed as assembled boulders of approximately 90 mm in size to prevent the shape of gravel mount against the supercritical flow passing through the mount under large discharges. In this experiment, the mounts were made of gravels with average sizes of 5.3 mm, 16.5 mm, 25.5 mm, 47.5 mm, and 92.1 mm on the basis of each gravel size averaged from their long sides, short sides, and height. The grain size distribution of the gravels used is summarized in Figure 1. In the case of gravels with average sizes of 5.3 mm and 16.5 mm, a coil with an inner diameter of 1.5 cm was inserted in the center of the channel at the mount installation stage to provide space for velocity measurement. In particular, in the case of the average size of 5.3 mm, a coil with an average size of 16.5 mm was covered around the coil to prevent small gravels from entering the coil (left side of Photo 1(a)). Installation intervals were approximately 30 cm. In the case of 25.5 mm, 47.5 mm, and 92.4 mm, coils were removed during the measurement phase. Depth and mount geometry were measured using a point gauge. The velocities were measured using an electromagnetic anemometer with an I-shaped probe of 4 mm diameter (sampling interval 50 ms, measurement time 30 s) produced by KENEK Ltd.. Video and photographs of the flow conditions were simultaneously recorded. The discharge was measured using a sharped edged suppressed weir (JIS standard) located at the downstream end of the channel.

(a) Gravel mount with averaged size 5.3 mm (inside region), crash stones of averaged size 92.1 mm (upstream installation part) and cobble stones of averaged size 47.5 mm (downstream installation area)

(b) Gravel mount with averaged size 16.5 mm (inside region), crash stones of averaged size 92.1 mm (upstream installation part) and cobble stones of averaged size 47.5 mm (downstream installation area)

(c) Gravel mount with averaged size 47.5 mm

(d) Gravel mount with averaged size 92.4 mm

Photo 1. Several types of gravel mount installed in a rectangular channel

Table 1. Experimental conditions

Case	Q (m^3/s)	h_u* (m)	Averaged Size (mm)	Sampling number
1	0.0174	0.233	5.3	379
2	0.0475	0.314	5.3	379
3	0.0174	0.255	16.5	122
4	0.0451	0.336	16.5	122
5	0.0174	0.247	25.5	100
6	0.0323	0.295	25.5	100
7	0.0475	0.331	25.5	100
8	0.0317	0.270	47.5	100
9	0.0174	0.219	92.1	100
10	0.0323	0.260	92.1	100
11	0.0475	0.297	92.1	100

*h_u is upstream depth at x = 0 m

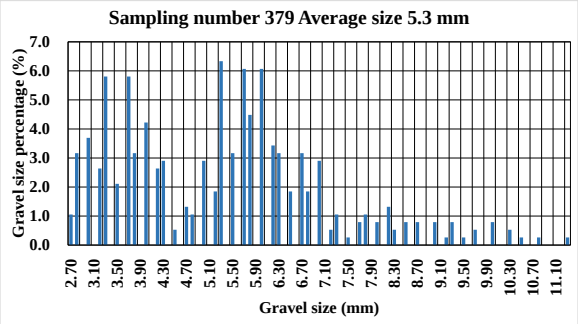

(a) Averaged size 5.3 mm

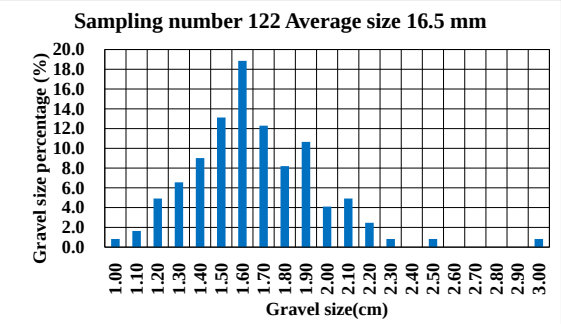

(b) Averaged size 16.5 mm

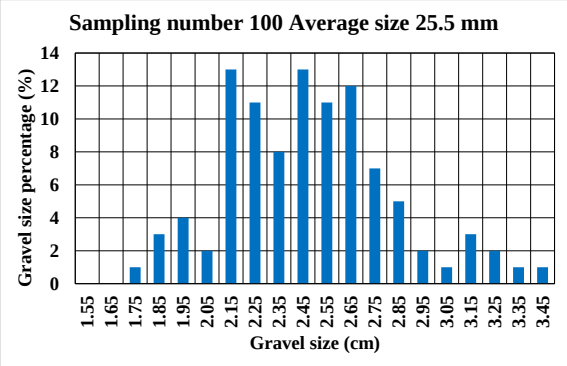

(c) Averaged size 25.5 mm

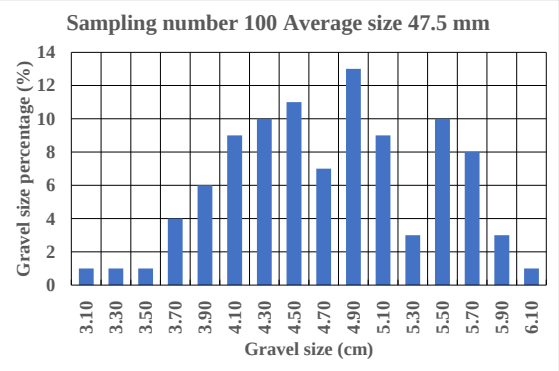

(d) Averaged size 47.5 mm

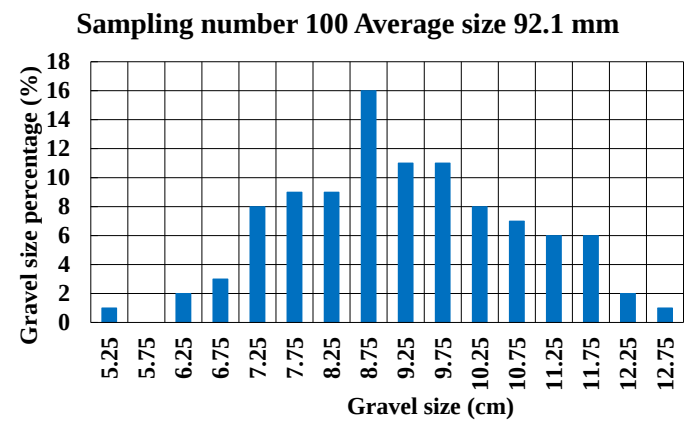

(e) Averaged size 92.1 mm

Figure 1. The grain size distribution of the gravels inside gravel mount

3. Flow Condition and Water Surface Profile Above Gravel Mount

Typical flow condition, in which Case 8 is represented, under discharge Q = 0.03231 m^3/s is shown in Photo 2. As shown in the photograph, the flow passing over the gravel mount transits from subcritical to supercritical flows in all cases. In all experimental conditions, the flow passing through the mount is not submerged, but a high velocity flow allows along the water surface, and the flow transits from supercritical to subcritical flows. Then, a supercritical flow is formed in the range of 100 cm < x < 250 cm. Further, a circulating flow is formed near the bottom of the downstream portion of the mount. An example of the water surface profile in the center of the channel (y = 20 cm) is shown in Figure 2. In the figure, x is the coordinate in the downstream direction with the origin at the upstream end of the mount, y is the coordinate in the transverse direction from the right sidewall of the channel, and z is the coordinate vertically above the reference channel bottom. As shown in the figure, the

unevenness of the water surface above the mount is affected by the shape of the mount. The effect of the unevenness of the mount on the shape of the water surface in the transverse direction is small.

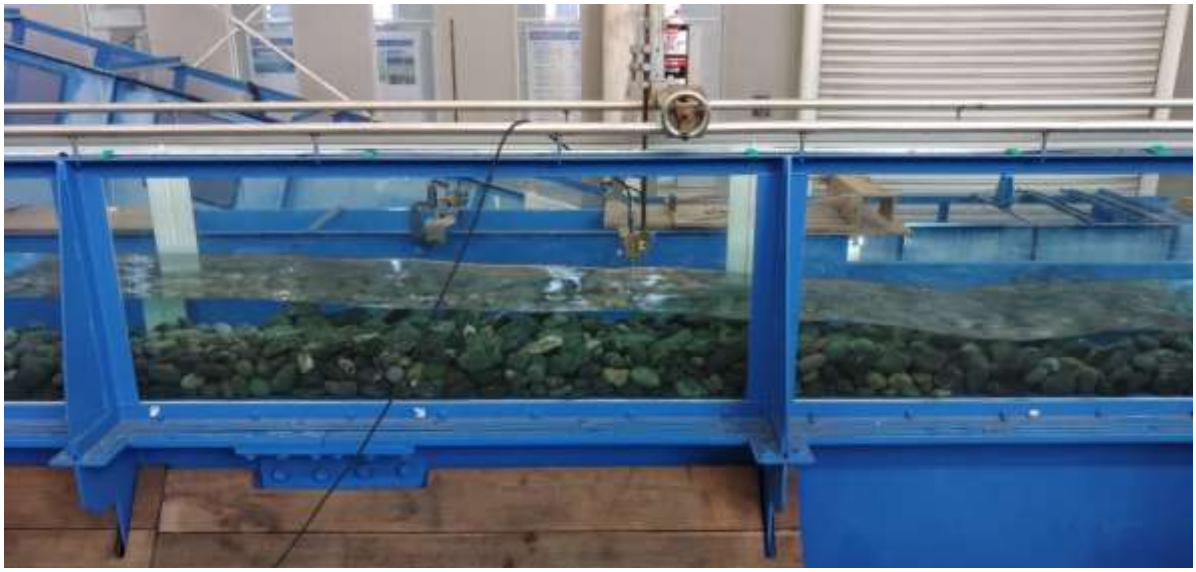

Photo 2. Flow condition for Case 8

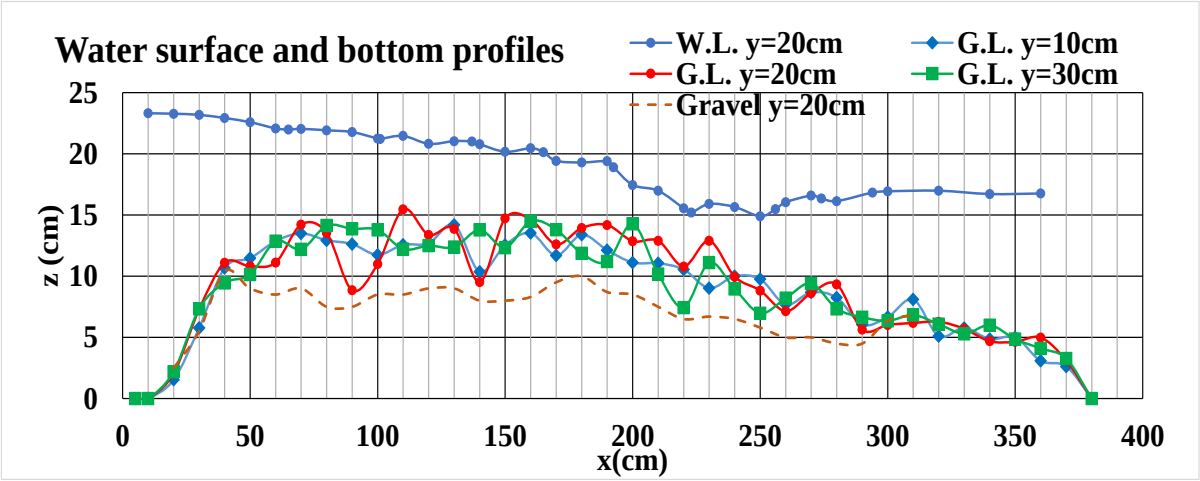

(a) Case 1

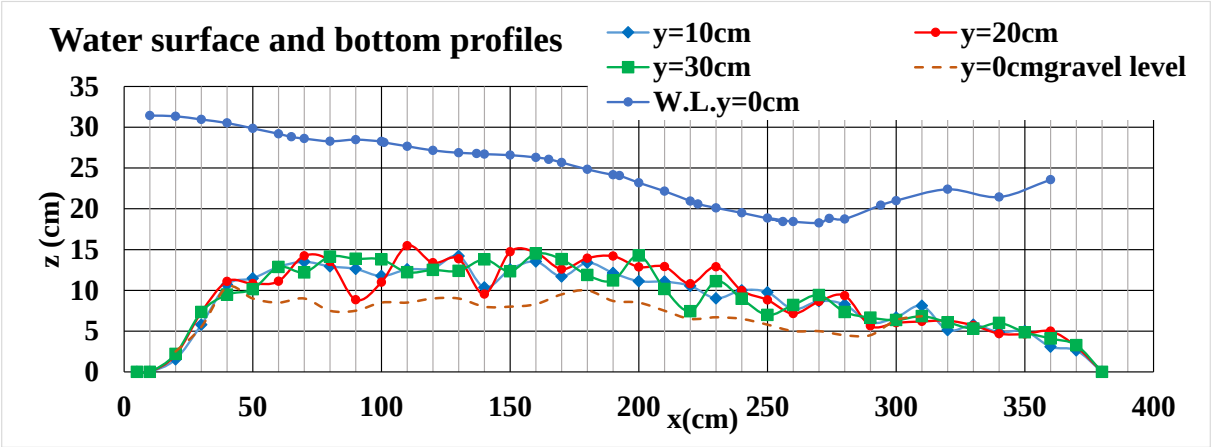

(b) Case 2

Figure 2. Example of water and gravel surface profiles in gravel mount

4. Velocity Profiles at Each Measurement Section in Installation Region of the Gravel Mount

The vertical distributions of time-averaged velocities and standard deviations at the central section of the channel (y = 20 cm) in the range of $0 < x \leq 210$ cm are shown in Figures 3, 4, 5, 6, and 7. In these figures, the blue dots and lines and the dark blue dots and lines indicate time-averaged velocity and standard deviation for x component, respectively. The orange dots and lines and the yellow dots and lines indicate the time-averaged velocity and standard deviation for y component, respectively. Since the main flow passing over the gravel mount is located near the water surface, the location of the maximum velocity for each cross-section is near the water surface. As shown in these figures, the magnitude of the time-averaged velocity in the subterranean water layer is small and its vertical variation is also small. Within the subterranean water layer, the more irregularly gravels are stacked, and the space between gravels is restricted, thus controlling turbulence. The magnitude of standard deviation in the subterranean water layer is smaller than that in the upper part of the gravel mount, because the turbulence in the surface part of the gravel mount may affect a turbulent flow between the assembled boulders. Furthermore, as the size of the gravels in the subterranean water increases, the magnitude and distribution of the time-averaged velocity may be affected by the flow between the gravels, depending on the shape of the assembled boulders and the local surface slope of the mount surface layer. In particular, the time-averaged velocity reaches up to 20 cm/s when the gravels in the subterranean are 47.5 mm and 92.1 mm in size (Figures 7 and 8).

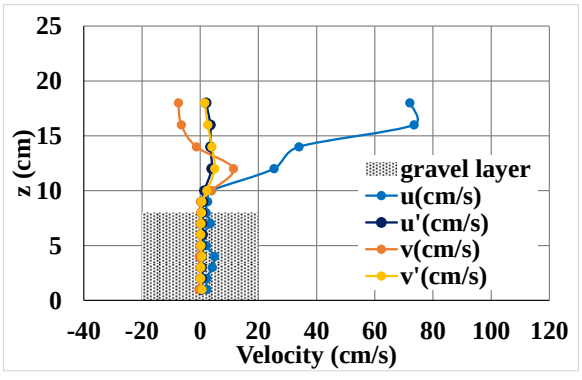

(a) x = 165 cm, Case 1

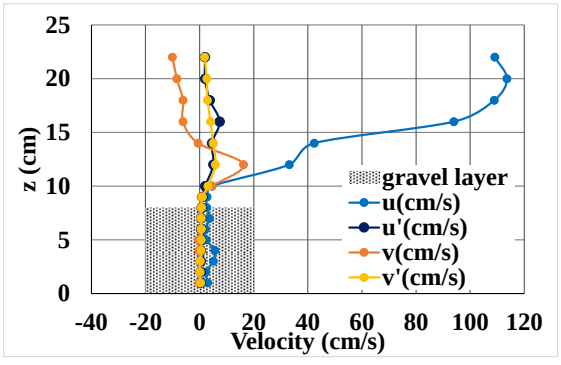

(b) x = 165 cm, Case 2

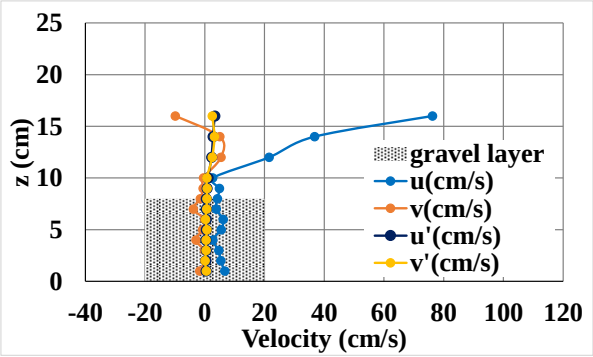

(c) x = 192.5 cm, Case 1

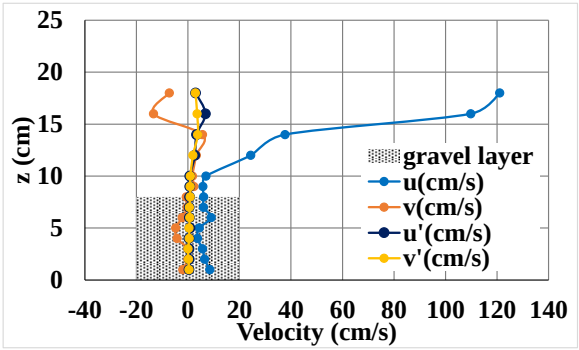

(d) x = 192.5 cm, Case 2

Figure 3. The vertical distributions of time-averaged velocities and standard deviations at the central section of the channel (Averaged size 5.3 mm)

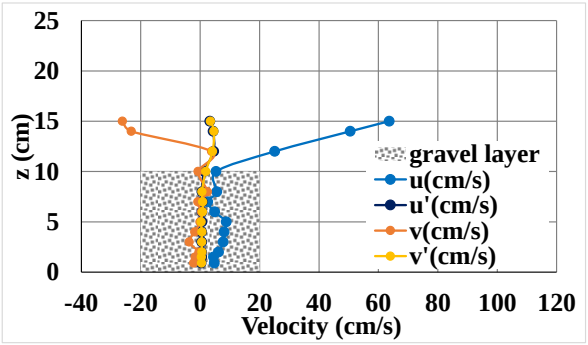

(a) x = 167 cm, Case 3

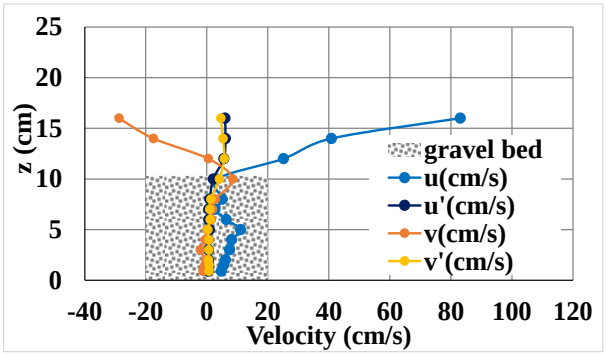

(b) x = 167 cm, Case 4

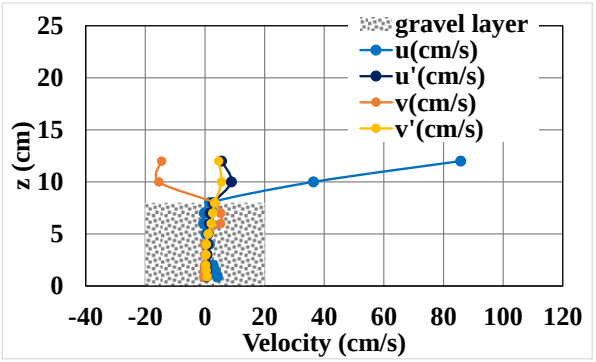

(c) x = 202 cm, Case 3

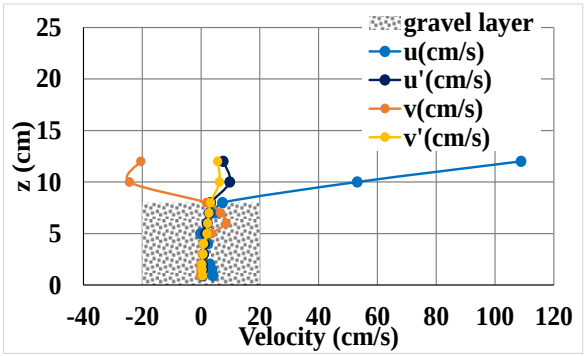

(d) x = 202 cm, Case 4

Figure 4. The vertical distributions of time-averaged velocities and standard deviations at the central section of the channel (Averaged size 16.5 mm)

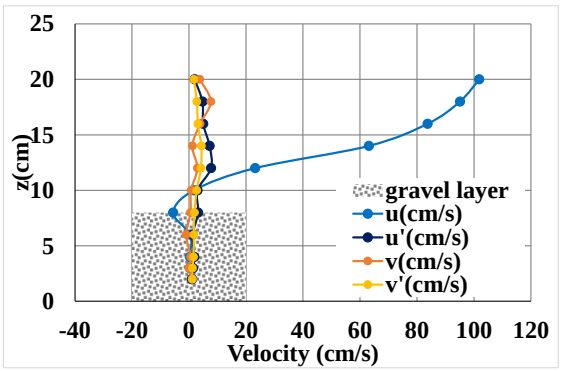

(a) x = 168 cm, Case 5

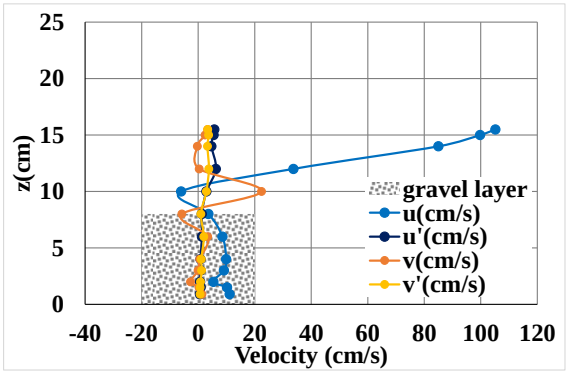

(b) x = 201 cm, Case 5

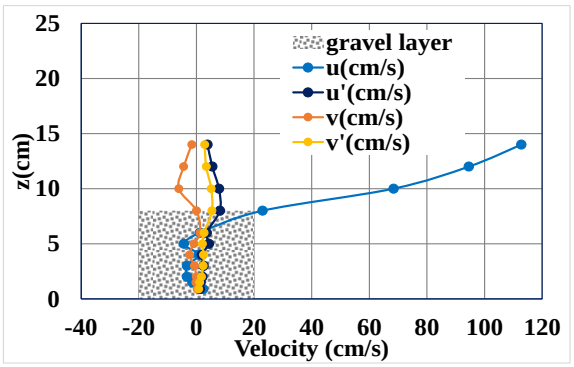

(c) x = 168 cm, Case 6

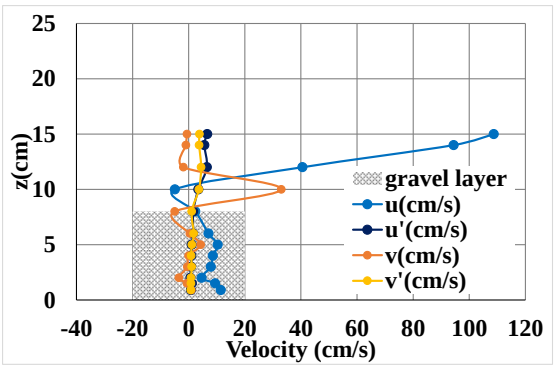

(d) x = 201 cm, Case 6

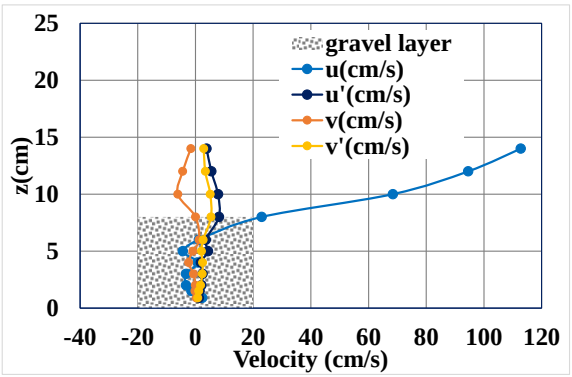

(e) x = 168 cm, Case 7

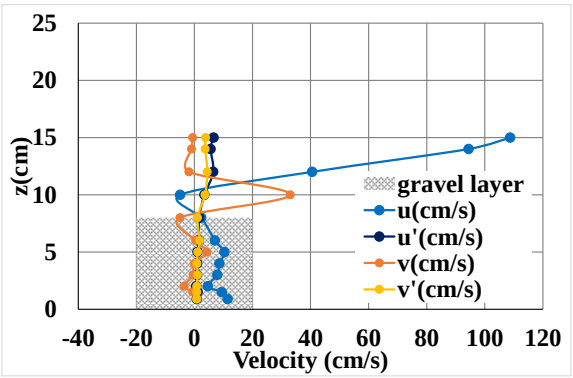

(f) x = 201 cm, Case 7

Figure 5. The vertical distributions of time-averaged velocities and standard deviations at the central section of the channel (Averaged size 25.5 mm)

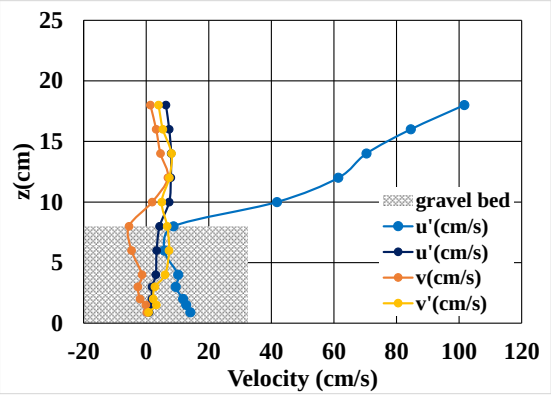

(a) x = 167 cm, Case 8

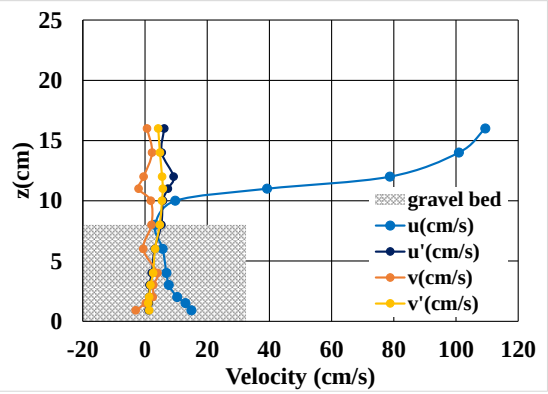

(b) x = 202 cm, Case 8

Figure 6. The vertical distributions of time-averaged velocities and standard deviations at the central section of the channel (Averaged size 47.5 mm)

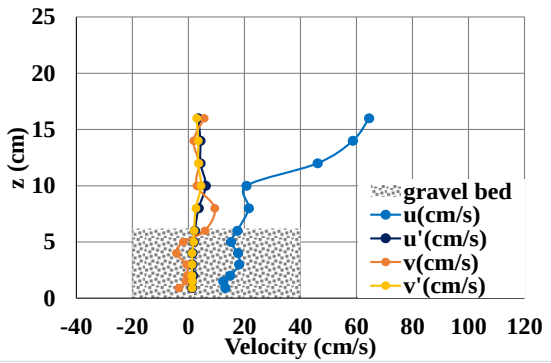

(a) x = 132.5 cm, Case 9

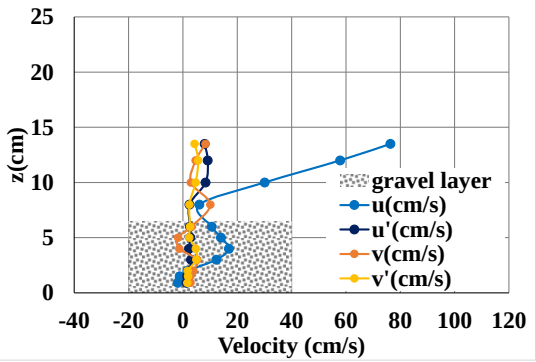

(b) x = 167.5 cm, Case 9

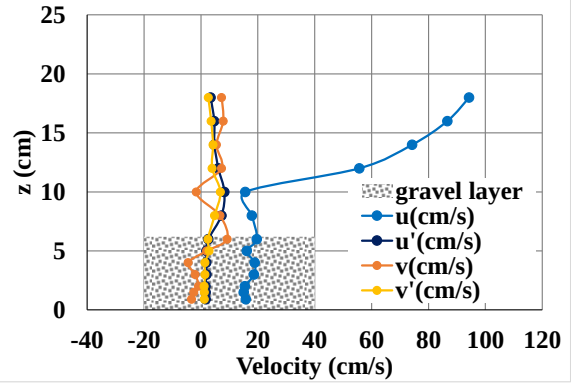

(c) x = 132.5 cm, Case 10

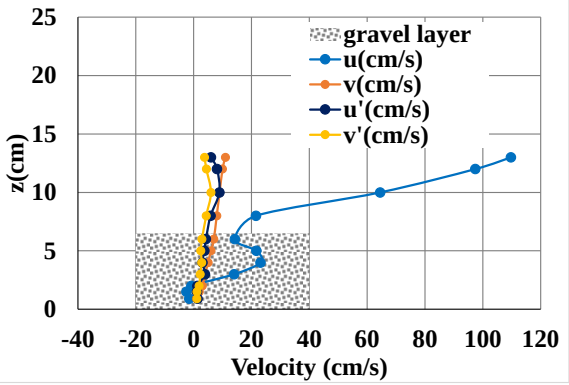

(d) x = 167.5 cm, Case 10

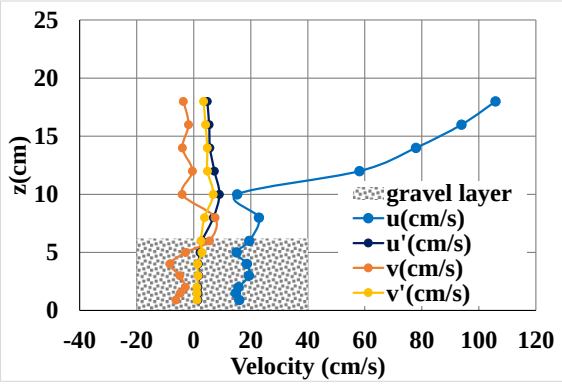

(e) x = 132.5 cm, Case 11

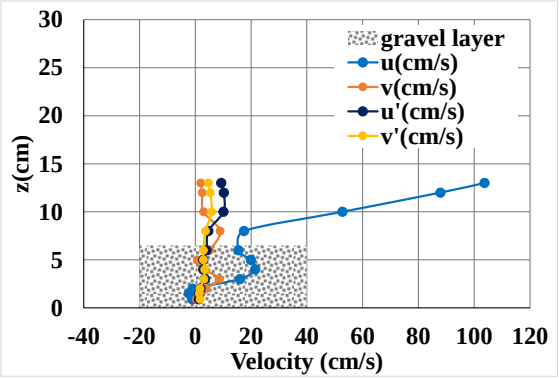

(f) x = 167.5 cm, Case 11

Figure 7. The vertical distributions of time-averaged velocities and standard deviations at the central section of the channel (Averaged size 92.1 mm)

Figure 8 shows the distribution of time-averaged velocity and standard deviation of the x component of each measured cross-section, together with the gravel mount configuration and water surface profile. The yellow arrows in the figure indicate the direction of flow into the subterranean layer due to the arrangement of the assembled boulders. The velocity in the upper part of the mount was measured up to the area where no separation with an air layer occurs at the detection point. As shown in this figure, the velocity near the bottom of the channel is larger than the velocity in the subterranean because the void between the channel and the gravels is larger than the void between the gravels, and the frictional resistance of the bottom is smaller. The boundary between the channel and the gravels corresponds to the case of a subterranean layer on smooth bedrock in a real river. The negative value of the time-averaged velocity in the subterranean layer is considered to be due to the effect of detachment caused by the way the boulders are assembled.

The vertical distribution of standard deviation at each measurement section indicates the local maximum standard deviation near the mount surface. The vertical profile of time-averaged velocity and the water surface profile indicate that the velocity of the flow along the bottom affects the flow passing over the top of the gravel mount. The larger size of the gravels may have affected the flow over the top of the mount because of the larger voids between the gravels.

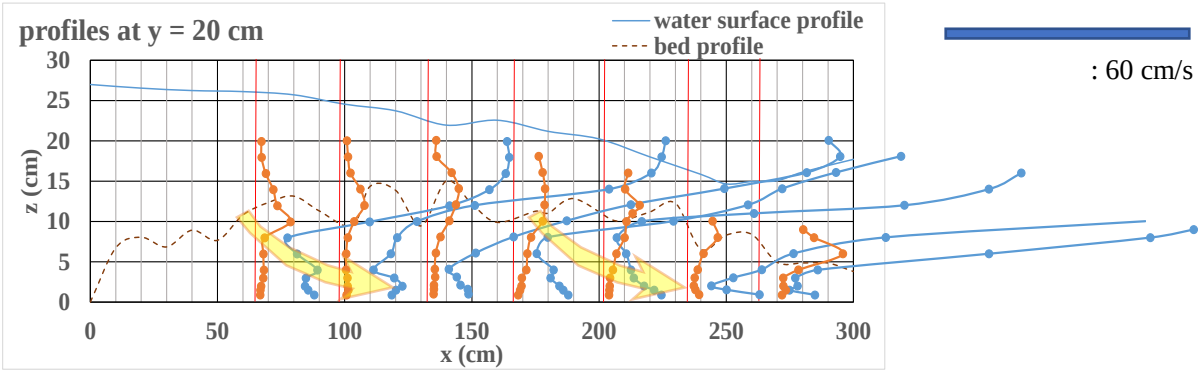

Figure 8. Vertical distributions of mean velocity and standard deviation for x-component in gravel mount (Averaged size 42.5 mm, Case 8)

5. Time-averaged Velocity and Standard Deviation Averaged Within the Subterranean Layer

The time-averaged velocities and standard deviations for x component within the subterranean layer are averaged for each measurement section, and they are denoted u_{ave} and u'_{ave}. The longitudinal changes of u_{ave} and u'_{ave} for the averaged gravel sizes of 5.3 mm, 16.5 mm, 25.5 mm, 47.5 mm and 92.1 mm are shown in Figures 9 to 13. As shown in these figures, the time-averaged velocity varies in the downstream direction, with little variation with discharge when the averaged size in the subterranean layer is small, with magnitudes ranging from

2 to 5 cm/s (Figures 9 and 10). For the averaged size of 25.5 mm, as the thickness of the subterranean layer decreases (for x ≥ 200 cm), the time-averaged flow velocity affects the flow between the gravels above the gravel mount (Figure 11). As the averaged size within the subterranean layer increases, the gaps become larger, showing differences due to the discharge, and the magnitude of the time-averaged velocity is also larger than for smaller averaged sizes (Figures 12 and 13). The downstream change of the averaged velocity u_{ave} depends on the configuration and gravel size of the gravel mount. The standard deviation u'_{ave} increases as the measurement cross section is located downstream, but the downstream change of the averaged standard deviation u'_{ave} is smaller than that of the averaged velocity u_{ave}, about 5 cm/s at most. For the averaged size of 47.5 mm, the averaged velocity u_{ave} is 10-15 cm/s, and the averaged velocity decreases with downstream direction up to x < 210 cm. Compared to the case with the averaged size of 16.5 mm, the downstream change of u_{ave} is different and the magnitude of the velocity is about two to three times greater. This might be caused by the larger velocity in the subterranean layer near the bottom and the larger gap between the gravels than in the 16.5 mm case.

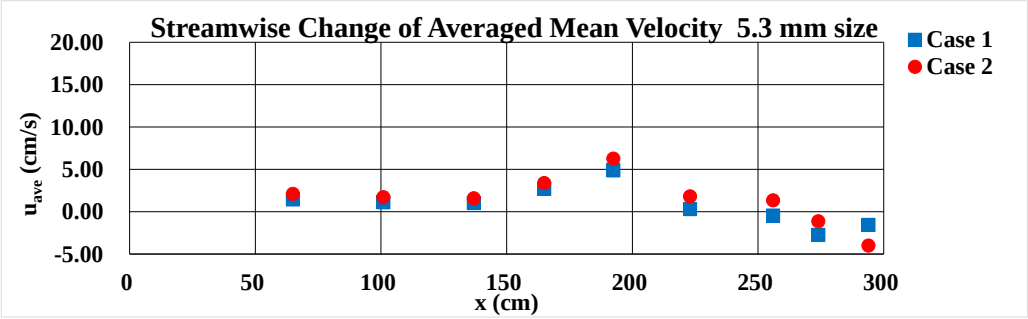

(a) Averaged value of mean velocity for x component at each measurement section

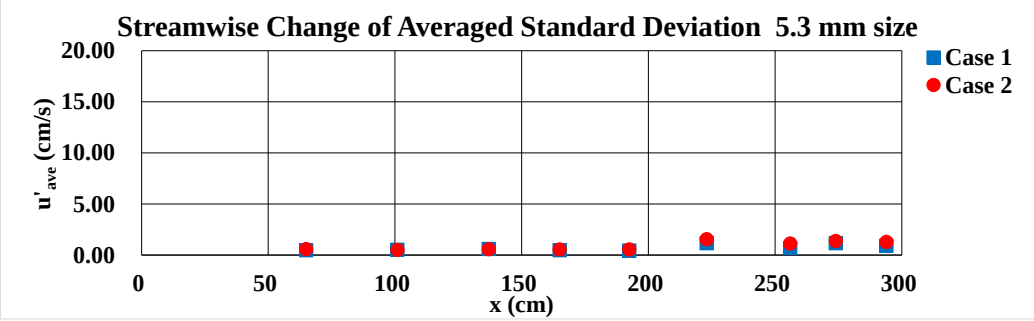

(b) Averaged value of standard deviation for x component at each measurement section

Figure 9. Stream-wise change of averaged value for Averaged size 5.3 mm

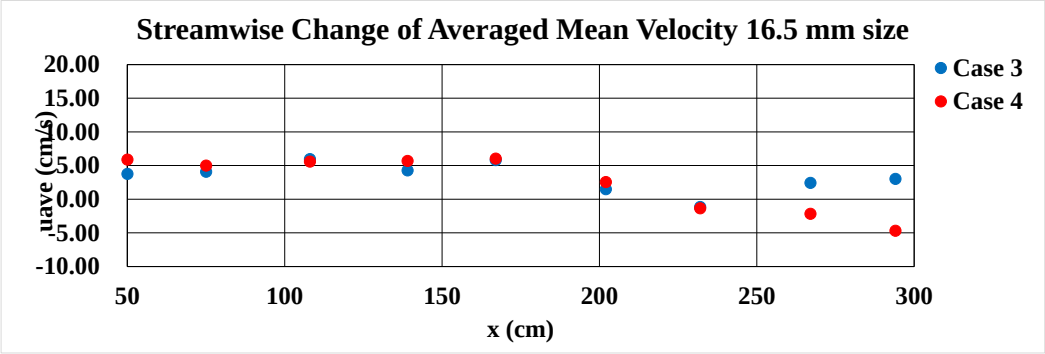

(a) Averaged value of mean velocity for x component at each measurement section

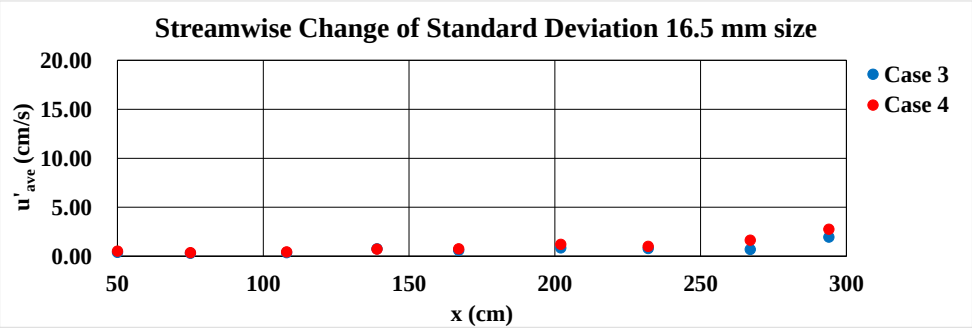

(b) Averaged value of standard deviation for x component at each measurement section

Figure 10. Stream-wise change of averaged value for Averaged size 16.5 mm

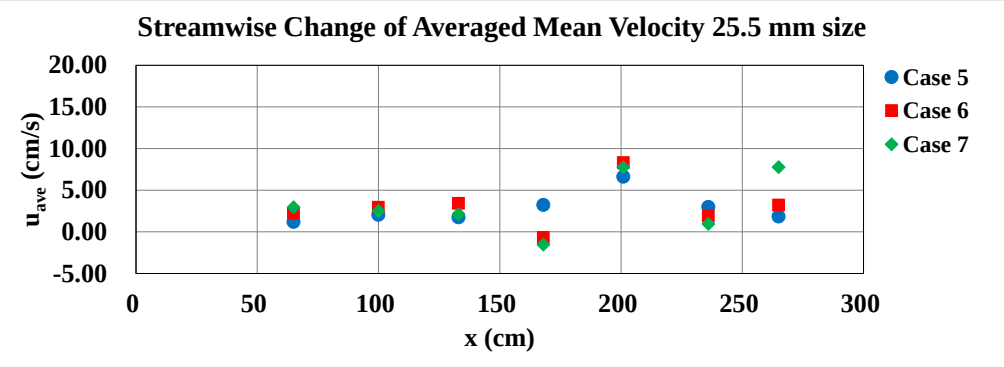

(a) Averaged mean velocity for x component

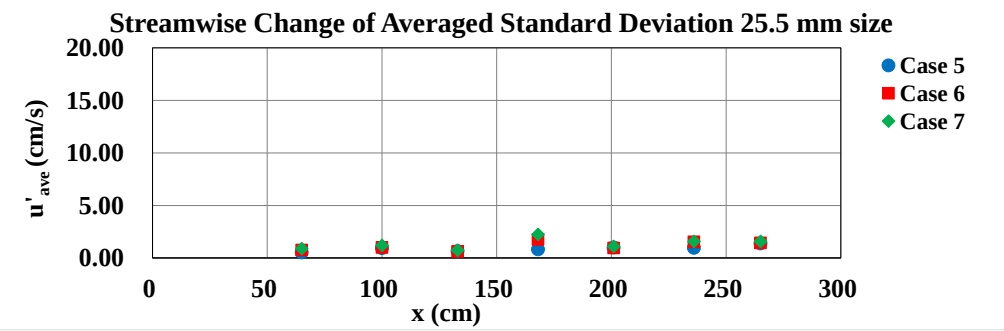

(b) Averaged standard deviation for x component

Figure 11. Stream-wise change of averaged value for Averaged size 25.5 mm

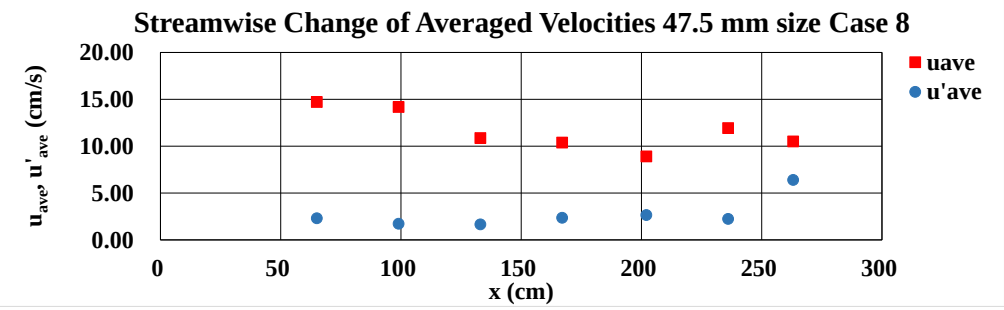

Figure 12. Stream-wise change of averaged value for Averaged size 47.5 mm

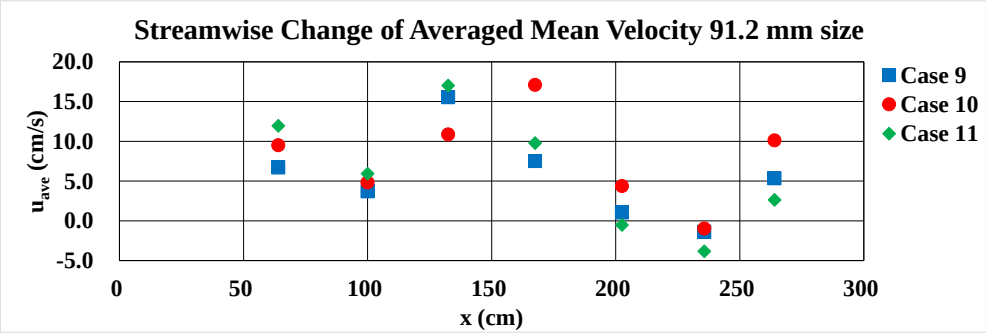

(a) Averaged mean velocity for x component

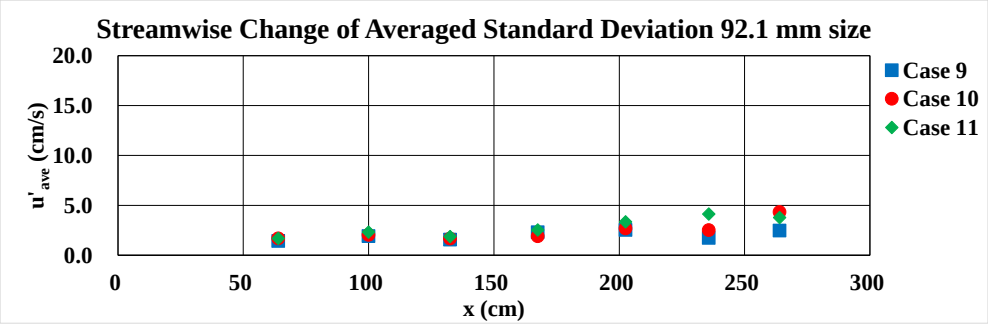

(b) Averaged standard deviation for x component

Figure 13. Stream-wise change of averaged value for Averaged size 92.1 mm

Comparing the case with the averaged size of 5.3 mm and the case with 16.5 mm in the x < 150 cm range, the value of the averaged time-averaged velocity is around 5 cm/s for the averaged size of 16.5 mm and around 2 cm/s for the case with 5.3 mm. As for the standard deviation, for gravels with mean diameters of 47.5 mm and 92.1 mm, values between 2 and 3 cm/s are obtained for x < 210 cm, as shown in Figures 13 and 14. Both cases with mean gravel diameters of 5.3 mm, 16.5 mm, and 25.5 mm show values of about 1 cm/s for x < 210 cm. The standard deviation (turbulence intensity) is less affected by the gap size and gravel size than by the time-averaged velocity in the subterranean for mean diameters between 5.3 and 25.5 mm.

Figure 14 shows the variation of time-averaged velocity and standard deviation with average diameter within the subterranean layer. Here, the time-averaged velocity and standard deviation evaluated at each measured cross-section where the flow on the gravel mount transits from subcritical to supercritical flows are shown as the overall average values. As shown in the figure, the trend of change is different at the boundary of the mean diameter of 30 mm. For averaged sizes between 5.3 mm and 25.5 mm, the time-averaged velocities and standard deviations are of similar magnitude, while for averaged sizes between 47.5 mm and 92.1 mm, the mean values of the time-averaged velocities and standard deviations are larger than those for averaged sizes between 5.3 mm and 30 mm, with the mean time-averaged velocity around 12 cm/s and the standard deviation around 2.5 cm/s.

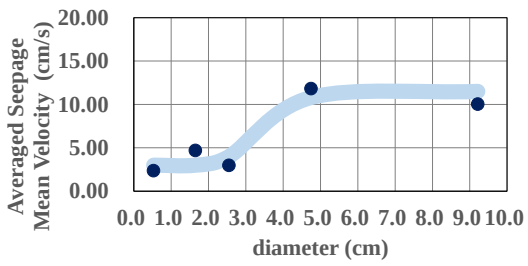

(a) Averaged mean velocity for x-component

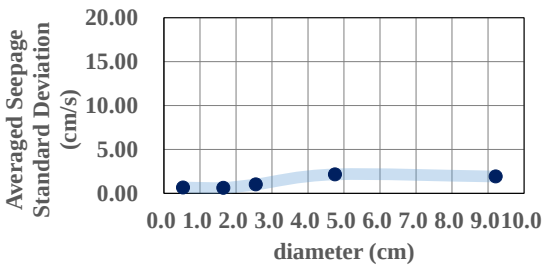

(b) Averaged standard deviation for x-component

Figure 14. Variation of mean velocity and standard deviation averaged inside the gravel mount by averaged size

6. Discussion

In Japan, there are field cases in which super dikes with consecutively assembled boulders were installed in the outer bank side of curved river in accordance with the suggestion of Yasuda, one of the authors of this paper. The example is shown in Photo 3. By installing groynes with the assembled boulders, the outer bank side is not eroded, and transported gravels naturally accumulates around the super dikes, forming a subterranean layer due to sand and gravel. This formation provides a habitat for aquatic animals. In addition, the assembled boulders provide shelter for aquatic animals, which use the area both during normal water and during floods. During times of drought, the subterranean water flow functions to regulate water temperature. In Japan, spawning beds for Ayu fishes are artificially created by using river stones (boulders). Most of the stones for the formation of the spawning bed are washed away during floods and cannot be regenerated, because the formation is based on experience without stabilization of basic structure during flood stages. As shown in this experiment, when the flow is over the gravel mount, the difference in water level and the local change in water surface gradient can be obtained, making it possible to artificially form subterranean water flow. In addition, the basic structure of the subterranean layer should be stabilized during flood stages.

The velocities of subterranean water flow, groundwater flow, and seepage flow are often evaluated indirectly based on the water surface gradient and hydraulic conductivity, but indirect evaluation does not provide accurate estimates because the flow in the subterranean layer has low turbulence and varies with the gaps and irregular spaces between gravels. From the results of time-averaged velocity and turbulence (standard deviation) in the subterranean layer for different sizes of gravels, it is possible to estimate the type of subterranean water flow formed by the grain size distribution of the depositing gravels and the difference in water level. The velocity in the subterranean layer can also be estimated. It is possible to estimate the possibility that the subterranean water flow might be controlled in the space between the large gravels and that it becomes a refuge for aquatic organisms in the area where the assembled boulders are set up, as shown in Photo 3.

(a) Super dikes of assembled boulders installed in Sakagawa river, Shizuoka Pref.

(b) Super dikes of assembled boulders installed in Kanna river, Gunma Pref.

(c) Sediment of gravels transported around super dike of consecutively assembled boulders

Photo 3. Transported gravels around super dikes of consecutively assembled boulders

7. Conclusion

The flow passing over the gravel mount shown in Photo 1 was formed, and five types of gravels with the grain size distribution shown in Figure 1, with average sizes of 5.3 mm, 16.5 mm, 25.5 mm, 47.5 mm, and 92.1 mm, were used to devise a way to measure the flow velocity when subterranean water flow is formed in the mount.

The velocity field in the subterranean layer was investigated under the experimental conditions shown in Table 1. It was confirmed that the gravel mount was always stable even if the discharge was increased. The flow passing over the gravel mount is formed to be the transition from subcritical to supercritical flow in the gravel mount, and to be the transition from supercritical to subcritical flows downstream of the gravel mount. The main flow follows the water surface at the downstream part of the gravel mount. In this case, the water surface profile of the flow over the gravel mount changes locally due to the unevenness of the gravel on the surface of the gravel mount. Flow velocities were measured in the center of the channel and time-averaged velocities and standard deviations were calculated. The results showed that both time-averaged velocities and standard deviations in the subterranean layer were controlled compared to those above the gravel mount, and the standard deviation results indicated that turbulence was controlled in all five types of gravels used. Regarding the time-averaged velocity, it was shown that the magnitude of the velocity within the subterranean layer increases by a factor of about four on the boundary of an average size of 30 mm. In other words, the magnitude of time-averaged velocity directly affects the arrangement of gravels in the mount surface layer when the space between gravels exceeds a certain degree. Since the space between the gravels is not penetrable, the turbulence does not increase and the standard deviation varies from 1 cm/s to 2.5 cm/s, averaged over the values in the subterranean layer by gravel size. The results of the authors' study indicate that it is possible to artificially control subterranean flow conditions depending on how the gravel size and water surface gradient are set. For example, it is possible to plan, design, and construct a river environment that is suitable for the circulation of flow in an artificial wand and for the growth of spawning and juvenile fishes as the formation of subterranean flow. It should be noted, however, that if the space between the gravels becomes too large, the flow velocity with turbulence will increase and sand and gravel will be sucked out.

In the future, the elucidation of local flows with various subterranean flows may be useful for improving the river environment in a wide range of areas. The authors are confident that the results of their study will be the first step in this direction.

References

Fukuoka, S., & Tabata, K. (2018). Index governing the seepage flow and dynamic similarity condition of levee failure due to seepage flow: seepage flow number and levee vulnerability index. *Journal of JSCE (Japanese Society of Civil Engineers) BI (Hydraulic Section), 74*(5), I.1435-I.1440 (in Japanese). https://doi.org/10.2208/jscejhe.74.5_I_1435

Ghasemizade, M., & Schirmer, M. (2013). Subsurface flow contribution in the hydrological cycle: lessons learned and challenges ahead—a review. *Journal of Environmental Earth Science, Special Issue, Springer, 69*, 707-718. https://doi.org/10.1007/s12665-013-2329-8

Han, Z., Chen, X. Y., Huang, Y. H., Huang, Y., Luo, B., Xing, H., & Huang, Y. (2020). Effect of slope gradient on the subsurface water flow velocity of sand layer profile. *Journal of Mountain Science, 17*(3), 641-652. https://doi.org/10.1007/s11629-019-5644-z

Kawanishi, R., & Inoue, M. (2018). Hyporheic zone as a fish habitat: ecological significant of vertical hydrological connectivity. *Journal of Groundwater Hydrology, 60*(2), 157-167. https://doi.org/10.5917/jagh.60.157

Nagai, S., Obana, M., & Chibana, T. (2013). The analysis of subsurface flow characterized by gravel bar shapes and the property. *Journal of River Engineering, JSCE, 19*, 555-560. (in Japanese)

Orchard, E. R. (1988). New method for measuring water seepage through salmon spawning gravel. *United States Department of Agriculture, Forest Service*. https://doi.org/10.2737/PNW-RN-483

Piccoli, B. P., & Yasuda, Y. (2023). Alternated gravel mounts with artificial assembled boulders reinforcement inside channelized rivers. *Journal of Environmental Science Studies, 6*(1), 26-35. https://doi.org/10.20849/jess.v6i1.1352

Schirmer, M., Luster, J., Linde, N., Perona, P., Mitchell, D. A. E., Barry, A. D., & Durisch-Kaiser, E. (2013). Morphological, hydrological, biogeochemical changes and challenges in river restoration – the Thur river case study. *Hydrology and Earth System Sciences Discussions, 18*, 2449-2462. https://doi.org/10.5194/hessd-10-10913-2013

Wheaton, M. J., Pasternack, B. G., & Merz, E. J. (2004). Spawning habitat restoration -I. Conceptual approach and methods. *International Journal of River Basin Management, 2*(1), 3-20. https://doi.org/10.1080/15715124.2004.9635218

Wroblicky, G. J., Campana, M. E., Valett, H. M., & Dahm, C. N. (1998). Seasonal variation in surface-subsurface water exchange and lateral hyporheic area of two stream-aquifer systems, *Water Resources Research, 34*(3), 317-328. https://doi.org/10.1029/97WR03285

Yasuda, Y., & Uemura, M. (2023). Experimental Investigation on Velocity Fields of Seepage Flow Inside Gravel Mount. *Journal of Environmental Science Studies, 6*(2), 14-25. https://doi.org/10.20849/jess.v6i2.1373

Yasuda, Y., Yasuda, K., & Piccoli, P. B. (2024). River Improvement, *Chapter 22, Fisheries Science Series, Springer, Editors: Tsukamoto, K., Kuroki, M., & Watanabe, S.*, 293-302, ISBN 978-981-99-5692-0 (eBook). https://doi.org/10.1007/978-981-99-5692-0

Zhang, H., & Chanson, H. (2015). Free-surface and seepage bubble flows on a gabion stepped spillway weir: experimental observations. *IAHR World Congress.* Retrieved from https://www.iahr.org/library/infor?pid=7754